

# Repolarization Gradients Alter Post-infarct Ventricular Tachycardia Dynamics in Patient-Specific Computational Heart Models

Eric Sung<sup>1,2</sup>, Adityo Prakosa<sup>1,2</sup>, Natalia A. Trayanova<sup>1,2</sup>

<sup>1</sup>Department of Biomedical Engineering, Johns Hopkins University, Baltimore, MD, USA

<sup>2</sup>Alliance for Cardiovascular Diagnostic and Treatment Innovation, Johns Hopkins University, Baltimore, MD, USA

## Abstract

*Repolarization heterogeneity contributes to ventricular tachycardia (VT) arrhythmogenesis but the impact of repolarization gradients on post-infarct VT dynamics is not well-characterized. The goal of our study is to assess the effects of repolarization gradients on post-infarct VT dynamics using patient-specific heart models. Baseline models were reconstructed along with the patient-specific scar and infarct border zone from imaging. Models with action potential duration (APD) gradients along apicobasal (AB) and transmural (TM) axes were also reconstructed. Rapid pacing was used to induce VTs. The resultant VT dynamics (inducibility, re-entry pathway, and the exit site) were assessed. Repolarization gradients did not impact VT inducibility but did alter both the re-entry pathway and exit site location due to modulations in unidirectional conduction block. Both AB and TM APD gradients alone were also sufficient for inducing these changes in VT dynamics. Lastly, APD gradients revealed multiple distinct morphologies that used similar conducting channels in the patient-specific substrate. These results highlight how the interplay between repolarization gradients and the patient-specific substrate can have consequences on post-infarct VT dynamics.*

## 1. Introduction

Ventricular tachycardia (VT) is a life-threatening arrhythmia that increases the morbidity and mortality of post-infarct patients. Despite significant improvements in clinical therapies such as catheter ablation, VT recurrence rates remain unacceptably high in part due to an incomplete understanding about the complex pathophysiology of the arrhythmogenic substrate.

Repolarization dispersion has long been recognized to be involved in VT arrhythmogenesis. Repolarization gradients, heterogeneities in repolarization dispersion, are known to exist in the human heart<sup>1,2</sup> and can be exacerbated during sympathetic stimulation.<sup>3</sup>

Furthermore, repolarization gradients have been observed to be more prevalent in ICM patients with VT than ICM patients without VT.<sup>4</sup> Although it is apparent that repolarization heterogeneity is present and important in VT arrhythmogenesis, it is unknown how or if repolarization gradients influence post-infarct VT dynamics.

Biophysically detailed, computational modeling can provide mechanistic insights into VT dynamics that may not be easily discernible from experimental or clinical studies. The goal of the present study is to evaluate the impact of repolarization gradients on post-infarct VT dynamics using patient-specific computational heart models. These findings would provide useful clinical insights for VT ablation therapy because repolarization gradients are likely to be modulated by the patient's sympathetic tone, often altered intraprocedurally by physiological or pharmacological means.<sup>3</sup> Thus, understanding the resultant effects of repolarization gradients on post-infarct VT dynamics could ultimately inform and improve ablation strategies.

## 2. Methods

### 2.1 Model Reconstruction

3D late-gadolinium enhanced cardiac magnetic resonance (LGE-CMR) images were acquired from 7 post-infarct patients without implanted cardioverter defibrillators (ICD). The resolution for 6 images was 0.625 x 0.625 x 2.5 mm and 0.625 x 0.625 x 2.0 mm for the last image. Each myocardium was segmented, and scar and infarct border zone were identified as done in previous works.<sup>5,6</sup> Computational heart models were reconstructed from the segmented myocardium along with the patient-specific scar and infarct border zone distributions. To run simulations of cardiac electrical wave propagation, finite-element, biventricular meshes were generated. Cardiac fiber orientations were assigned on an element-wise basis, as done in previous works<sup>5,6</sup>. Electrical wave propagation simulations were executed by

solving the monodomain equations using the Cardiac Arrhythmia Research Package (CARP) software.

## 2.2 Model Electrophysiological Properties

For baseline models, electrophysiological properties were assigned to non-injured myocardium and infarct border zone as done in previous works.<sup>5</sup> Scar was assumed to be non-conducting across all models.

Repolarization gradients were created by modifying the action potential duration (APD) by scaling the slowly activated delayed rectifier potassium ( $I_{Ks}$ ) current along both the apicobasal (AB) and transmural (TM) axes.<sup>7</sup> This APD gradient (AB-TM) was assessed because it is known to exist physiologically.<sup>1,2</sup> From base to apex and from endocardium to epicardium, the  $I_{Ks}$  current was scaled by a factor of 1 to 1.5 in accordance with previous literature.<sup>7</sup> Both scaling ranges were then multiplied together to achieve an  $I_{Ks}$  current scaling from 1 at the basal endocardium to 2.25 at the apical epicardium. To evaluate the individual effects of both the AB and TM repolarization gradients on VT dynamics, separate models with only AB and only TM APD gradients were also reconstructed.

Only  $I_{Ks}$  current in non-injured myocardium was scaled. The rationale for this choice was that the ionic current adjustments for the infarct border zone were made agnostic of the location or the distribution of the infarct.

## 2.3 VT Induction Protocol

Baseline VTs were induced via pacing pulse trains from the right ventricular apex, similar to standard clinical induction protocols used during ablation procedures. The pacing consisted of a series of 6 stimuli (S1) delivered at a fixed basic cycle length (BCL) followed by up to 3 extra premature stimuli. For each pacing location, two different S1 basic cycle lengths were tested (600 ms and 350 ms) to assess the substrate arrhythmogenicity more comprehensively.

Stimulus protocols that successfully induced VT in baseline ventricular models were then applied to AB-TM models. Because the APD gradients change the tissue effective refractory period, the earliest possible timings premature stimuli are likely to change for models with APD gradients. To account for this change, two induction protocols were considered for APD gradient models. First, the exact timings of stimuli from protocols that induced VTs in baseline models were re-applied to models with APD gradients. This first protocol will be referred to as the exact timed stimulus (XTS) protocol. Secondly, the earliest possible timings of stimuli were identified and applied in APD gradient models. This

second protocol will be called the earliest timed stimulus (ETS) protocol. This same procedure was applied to AB only and TM only models as well to dissect the contributions of each APD gradient on VT dynamics. VTs were defined as having at least two re-entrant cycles, the same definition as used in previous works.<sup>5,6</sup> VT

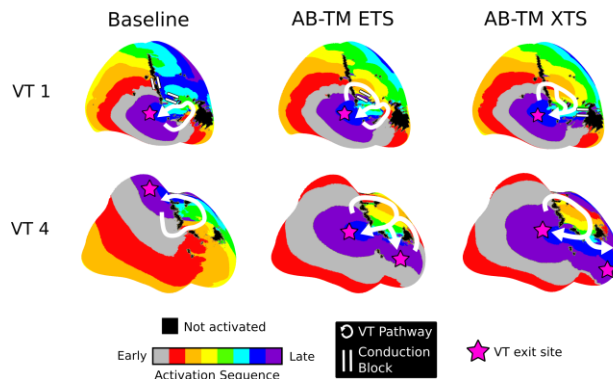


Figure 1: Examples where APD gradients altered VT dynamics. The VT pathway is shown in white, areas of conduction block are shown with two white lines, and the VT exit sites are denoted with pink stars.

dynamics (inducibility, re-entry pathway, and exit site location) were then compared between models.

## 3. Results

### 3.1 Repolarization gradients altered re-entrant pathways and VT exit sites, but not inducibility.

Ten VTs were induced across the 7 baseline models. In APD gradient models, 7 VTs were induced across both the ETS and XTS protocols. The inducibility of AB-TM models was not significantly different than baseline models ( $p > 0.05$ , Fisher's test). These results suggest that repolarization dispersion may not have a pronounced impact on arrhythmogenicity. VTs induced in AB-TM models used different re-entrant pathways than VTs induced in baseline models ( $p < 0.05$ , Fisher's test). For both the AB-TM XTS-induced and ETS-induced VTs, 6/7 of the VTs had different conduction pathways.

Figure 1 shows examples of how repolarization gradients affect the VT re-entrant pathway and VT exit sites by changing locations of conduction block. For instance, baseline model VT 1 had two areas of conduction block (Fig.1, top row). In AB-TM models, both the ETS and XTS protocols induced VTs with double-loop type morphologies that had the same exit site as the baseline VT but utilized different pathways that were blocked in the baseline model (Fig. 1, top center and right).

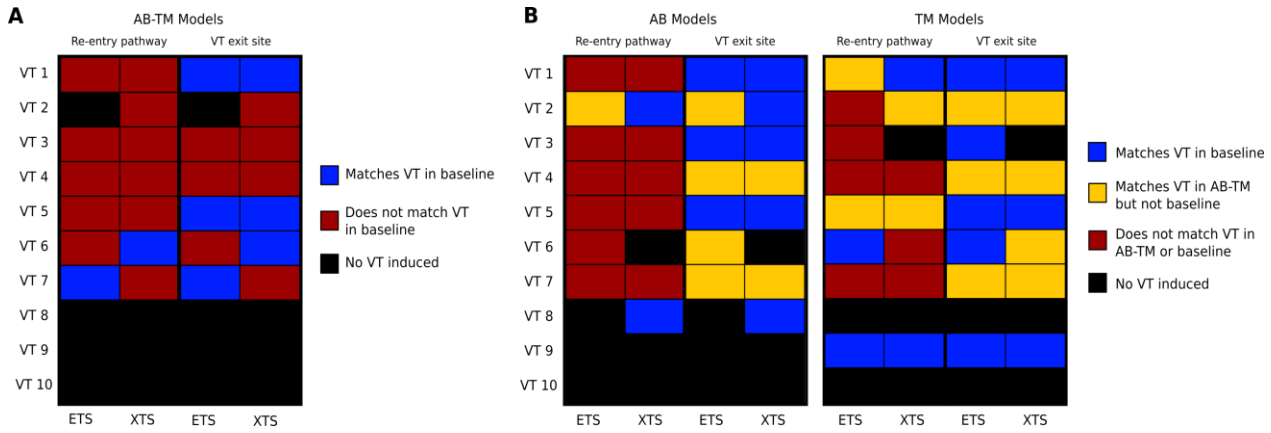


Figure 2: Comparison of re-entry pathway and VT exit sites across APD gradient models. A: Comparisons of re-entry pathway and VT exit sites between AB-TM and baseline models. Each row represents a different VT. Blue means the two were consistent, red means that the two were not consistent, and black means no VT was induced. B: Comparisons of re-entry pathway and VT exit sites between AB and TM with baseline and AB-TM models. Blue means there was a match with baseline models, red means there was no match with either baseline or AB-TM models, orange means there was a match with AB-TM models but not baseline models, and black means there was no VT induced.

Most VT exit sites in AB-TM APD gradient models were different than VT exit sites in baseline models. Whereas 3/6 AB-TM ETS-induced VTs had similar VT exit sites as baseline VTs, only 2/7 AB-TM XTS-induced VTs had the same exit site as baseline VTs. Baseline VT 4 had a single-loop morphology that entered through the mid interventricular junction and exited towards the right ventricular outflow tract (Fig.1, bottom). However, VT 4's entrance and exit sites were reversed in the AB-TM model (Fig.1, bottom). Moreover, both ETS and XTS-induced VTs had a second exit site towards the apex.

These examples demonstrate how repolarization gradients in conjunction with premature stimulus timing modulate conduction block, and hence determine the resultant re-entrant pathway and VT exit site.

### 3.2 AB or TM APD gradients alone are sufficient to alter re-entrant pathways and VT exit sites.

Similar to AB-TM APD gradients, both AB only and TM only APD gradients affected locations of conduction block which subsequently altered the re-entrant pathway and exit site location. Figure 2 summarizes how VT re-entrant pathways in AB only and TM only models compare with re-entrant pathways in AB-TM and baseline models. Re-entrant pathways in both AB models and TM models were different than re-entrant pathways in baseline models ( $p < 0.05$ , Fisher's test) and in AB-TM models ( $p < 0.05$ , Fisher's test).

Most VT exit sites in AB and TM models were at different locations than baseline VT exit sites but were spatially concordant with VT exit sites in AB-TM models. AB ETS induced 4/7 VTs with different exit sites; contrarily, AB XTS induced only 2/7 VTs with different exit sites than baseline. For TM models, 3/8 ETS-induced VTs and 4/7 XTS-induced VTs had different exit sites than baseline. Thus, these results demonstrate how both

independent AB and TM repolarization gradients are sufficient to alter post-infarct VT dynamics by modulating locations of conduction block.

### 3.3 APD gradients revealed multiple VTs within the same conducting channels.

Figure 3 illustrates two models where multiple VT morphologies were uncovered within the same conduction channels through the various APD gradients and stimulus protocols. In model C, 5 different morphology types were identified (Fig.3 left). The first type of VT morphology was identified only in the baseline model with the re-entrant pathway completely contained within the inner loop of the circuit and exited through both sites 'a' and 'c' (Fig.3, left). Morphology types 2, 3, 4, and 5 had different permutations of entrances and exit sites at 'a', 'b', and 'c'.

For model D, morphology types 1 and 2 were the most common VTs observed (Fig.3, right). The first VT type entered through both sites 'b' and 'c' and exited via site 'a', whereas the second type entered through sites 'a' and 'c' and exited through site 'b' in a figure-of-eight configuration. Morphology types 3 and 4 had the reversed chirality of the first two morphology types, respectively.

Both models C and D demonstrate how the correct combination of repolarization gradients and premature stimulus timing can result in multiple VT morphologies manifesting within the same conducting channels in the patient-specific substrate.

## 4. Discussion and Conclusion

This study assessed the effects of repolarization gradients, in the form of APD gradients, on post-infarct VT dynamics using computational whole-heart models. Inclusion of APD gradients did not significantly affect

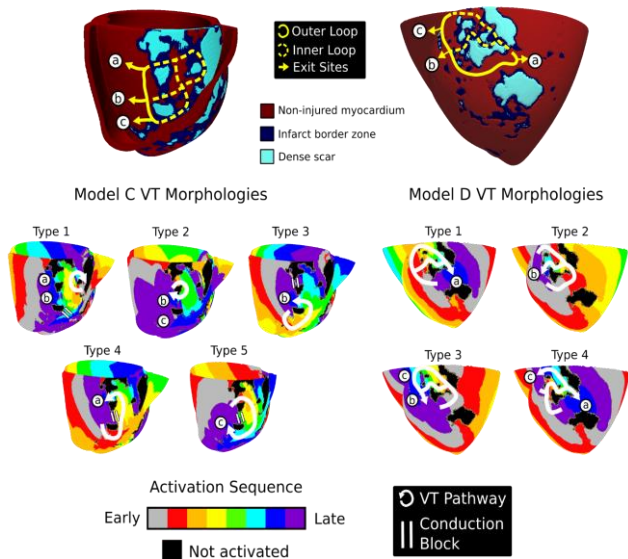


Figure 3: APD gradients reveal multiple morphologies within the same conducting channels. The yellow lines denote the possible conduction pathways; the solid yellow line is the outer loop, the dashed yellow line is the inner loop, and the arrowhead denotes the exit site. For both models, all exit site locations are denoted with the circled letters ‘a’, ‘b’, and ‘c.’

VT inducibility. However, in most patient-specific substrates, these APD gradients altered the VT pathway and the VT exit site location by modulating locations of unidirectional conduction block. Lastly, incorporating APD gradients unmasked multiple VT morphologies within the same conducting channels, highlighting the complex interdependence between electrophysiological heterogeneity and the patient-specific scar and infarct border zone distribution.

Catheter ablation, one of the major therapies for VT, relies on careful understanding of the post-infarct VT circuit to successfully eliminate substrate arrhythmogenicity.<sup>1</sup> Modulation of sympathetic tone such as with anesthesia and sympathomimetics can impact ventricular electrophysiology and arrhythmogenicity.<sup>1,2</sup> Increased sympathetic stimulation increases spatial dispersion of repolarization in infarcted hearts.<sup>1</sup> ICM patients with VT exhibit larger repolarization gradients than ICM patients without VT.<sup>4</sup> Our results are consistent with these findings and offers mechanistic insights into how different repolarization gradient can have a major impact on VT dynamics. Ablation strategies that target only a single part of the clinical VT circuit may neglect alternate pathways capable of harboring other distinct VTs that manifest under different electrical conditions. Thus, the patient’s current sympathetic state and repolarization dynamics, which could be assessed via electrocardiogram (ECG), should be considered during VT ablation to ensure that all possible VTs are eliminated.

Using computational whole-heart models, we characterized the effects of various repolarization gradients on post-infarct VT dynamics. Although repolarization gradients did not seem to impact VT inducibility and the VT circuit locations were unlikely to change, repolarization gradients altered both the VT pathway and VT exit site locations due to changes in the location of conduction block. Thus, repolarization gradients induced physiologically or pharmacologically via autonomic regulation could impact post-infarct VT dynamics and may need to be considered during ablation therapy to minimize VT recurrence.

## Acknowledgments

None

## References

- [1] Opthof, T., Coronel, R. & Janse, M. J. Is there a significant transmural gradient in repolarization time in the intact heart?: Repolarization gradients in the intact heart. *Circulation: Arrhythmia and Electrophysiology* vol. 2 89–96 (2009).
- [2] Glukhov, A. V. *et al.* Transmural dispersion of repolarization in failing and nonfailing human ventricle. *Circulation Research* 106, 981–991 (2010).
- [3] Ajjjola, O. A. *et al.* Sympathetic modulation of electrical activation in normal and infarcted myocardium: Implications for arrhythmogenesis. *American Journal of Physiology - Heart and Circulatory Physiology* 312, H608–H621 (2017).
- [4] Chauhan, V. S. *et al.* Increased ventricular repolarization heterogeneity in patients with ventricular arrhythmia vulnerability and cardiomyopathy: a human in vivo study. *Am J Physiol Heart Circ Physiol* 290, 79–86 (2006).
- [5] Prakosa, A. *et al.* Personalized virtual-heart technology for guiding the ablation of infarct-related ventricular tachycardia. *Nature Biomedical Engineering* 2, 732–740 (2018).
- [6] Sung, E. *et al.* Personalized Digital-Heart Technology for Ventricular Tachycardia Ablation Targeting in Hearts with Infiltrating Adiposity. *Circulation: Arrhythmia and Electrophysiology* (2020).
- [7] Keller, D. U. J., Weiss, D. L., Dossel, O. & Seemann, G. Influence of IKs heterogeneities on the genesis of the T-wave: A computational evaluation. *IEEE Transactions on Biomedical Engineering* 59, 311–322 (2012).

Address for correspondence:

Name: Eric Sung

Full postal address: 3400 N. Charles Street Hackerman Hall 216  
Baltimore, MD 21218

E-mail address: esung2@jhmi.edu